

Pulsed Laser Ablation of Soft Tissues, Gels, and Aqueous Solutions at Temperatures Below 100°C

Alexander A. Oraevsky, PhD, Steven L. Jacques, PhD,
Rinat O. Esenaliev, PhD, and Frank K. Tittel, PhD

Department of Electrical and Computer Engineering, Rice University, Houston, Texas 77251 (A.A.O., S.L.J., R.O.E., F.K.T.); Laser Biology Research Lab. UT/M.D. Anderson Cancer Center, 1515 Holcombe Boulevard, Houston, Texas 77030 (A.A.O., S.L.J.)

Background and Objective: It is desirable for laser microsurgical procedures to remove tissue accurately and with minimal thermal and mechanical damage to adjacent non-irradiated tissues. Pulsed laser ablation can potentially remove biological tissue with microprecision if appropriate irradiation conditions are applied. The major goal of this study was to determine whether laser ablation is possible at temperatures below 100°C. Another aim was to test thermoelastic and recoil stress magnitudes and to estimate their effects on phantom and biological tissue.

Study Design/Materials and Methods: Pulsed laser ablation of water (aqueous solution of potassium chromate) and water containing soft tissues (collagen gel and pig liver) irradiated under confined stress conditions was studied. The ablation mechanism and stages of the ablation process were determined based on time-resolved measurements of laser-induced acoustic waves with simultaneous imaging of the ablation process by laser-flash photography.

Results: This study reveals the important role of tensile thermoelastic stress, which produces efficient cavitation that drives material ejection at temperatures substantially below 100°C. Ablation thresholds for the aqueous solution, collagen gel, and liver were 20, 38, and 55 J/cm³, respectively, which correspond to temperature jumps of 5, 10, and 15°C. Two distinct stages of material ejection were observed: (1) initial removal of small volumes of material due to the rupture of single subsurface bubbles, (2) bulk material ablation in the form of jets produced by intense hydrodynamic motions formed upon collapse of large bubbles after coalescence of smaller bubbles. The duration of material ejection upon short-pulse ablation may vary from microseconds to sub-milliseconds, and depended on the mechanical properties of materials and the incident laser fluence.

Conclusion: Nanosecond laser ablation of water, gels, and soft tissue under confined-stress conditions of irradiation may occur at temperatures below 100°C. This ablation regime minimizes thermal injury to adjacent tissues and involves thermoelastic stress and recoil pressure magnitudes, which may be tolerated by tissues adjacent to an ablated crater. © 1996 Wiley-Liss, Inc.

Key words: laser-induced stress, cavitation, spallation, thermal explosion, acoustic transducer, flash photography

INTRODUCTION

Precise pulsed laser ablation of soft biological tissues with minimal thermal and mechanical damage to adjacent non-irradiated tissues is very

Accepted for publication January 30, 1995.

Address reprint requests to Alexander Oraevsky, Electrical Engineering Department, Rice University, P.O. Box 1892, Houston, TX 77251-1892.

attractive for microsurgical treatments of delicate human organs (eye, ear, brain, etc.). The full potential precision of tissue removal by laser pulses can be achieved if two conditions are satisfied: (1) the tissue temperature rise should be low and transient to avoid protein coagulation, and (2) the stress magnitude and gradient created by ablation recoil and propagated outside the irradiated volume should never reach the threshold for mechanical destruction of cells or tissue structures. In such a case, the dimensions of an ablated crater are defined by controlled parameters, and the diameter of a crater is very close to the diameter of the laser beam with a uniform (tophat) radial intensity distribution. The most reliable way to satisfy conditions (1) and (2) is to ablate tissue at temperatures below the point of protein coagulation and with relatively low-amplitude stress transients that do not yield shock waves. The aim of the present study was to describe the mechanism and necessary conditions of irradiation for ablation to proceed at temperatures below 100°C.

To date there have been a considerable number of experimental and theoretical attempts to evaluate ablation mechanisms for soft biological tissues under various irradiation conditions [see review in 1]. Effects of laser parameters on the magnitude and dimensions of thermal injury produced by laser ablation in biological tissues have been reported by many groups. Pulsed laser irradiation of tissues with microsecond and submillisecond pulses achieves ablation while avoiding diffusion of thermal energy outside the irradiated volume [2]. Such thermal confinement allows thermal injury of tissues adjacent to the ablation crater to be limited [3].

Application of even shorter pulses generated by Q-switched solid state and excimer lasers (1–100 ns) offers a uniquely “cold” ablation regime [4,5]. It has been demonstrated in several experimental and theoretical studies that short-pulse laser ablation has the advantage of being the least thermally damaging to adjacent tissue layers [3–9]. Because of a very high rate of laser energy conversion into heat in water containing biological media ($<10^{-9}$ s), nanosecond laser pulses are capable of creating a substantial thermal stress without a significant temperature rise. This phenomenon can be observed when a laser pulse heats tissue faster than the time it takes for the thermoelastic expansion of the heated volume to occur. These irradiation conditions are called *confined-stress conditions* in which stress does not propagate out of the irradiated volume during the

time of heat generation by the laser pulse. The product of light penetration depth, speed of sound, and laser pulse duration yields the dimensionless parameter of stress confinement, $\mu_{\text{eff}} c_s \tau_L$, which defines the degree of stress confinement upon laser heating. The threshold temperature rise for ablation of water and aqueous solutions under confined-stress irradiation conditions ($\mu_{\text{eff}} c_s \tau_L \ll 1$) was found to be only 5°C [8,9].

There is no published comprehensive experimental study on the subject of biological tissue ablation under confined-stress irradiation. Some data are evident for a “cold” cavitation-based ablation evoked by thermoelastic expansion [8–10]. Other experiments have demonstrated that the ablation-threshold temperature for nanosecond (excimer) lasers could be higher than 100°C [11–13]. The reasons why laser pulses with similar pulse length may or may not ablate tissue at temperatures below 100°C are discussed in the present paper. The major goal of this study was to answer the following two questions: What is the temperature of soft tissue ablation under confined stress conditions of irradiation? What are laser irradiation parameters for ablation at temperatures below 100°C, if it all possible?

MATERIALS AND METHODS

Aqueous Solutions, Gels, and Liver Tissue

An aqueous solution of potassium chromate (K_2CrO_4) was employed to study the ablation of clear, homogeneously absorbing liquid. Optical and chemical properties of aqueous K_2CrO_4 were studied prior to ablation experiments. A solution of 1 g K_2CrO_4 in 100 ml of distilled water yields an absorption coefficient of 300 cm^{-1} at a 355-nm wavelength. Dilution of the initial solution allows manipulation of the light penetration depth in media under study. In contrast to organic dye solutions commonly used in similar studies, four important advantages of potassium chromate were found: (1) Potassium chromate solution absorbs visible and near-UV photons, and variation of the solution concentration allows the realization of any desired penetration depth of light and stress confinement parameter; (2) this solution is practically nonfluorescent and, therefore, the total absorbed laser energy is converted into heat; (3) this solution is photochemically stable and its optical properties are not altered at high laser irradiance; and (4) this solution has an optical transmission window in the yellow-red spectral range, so that the ablation process above and be-

neath the irradiated surface of either water or gel can be visualized by laser-flash photography. Before each experiment solutions were filtered through μ Star-LB™ 0.22 μ m filters (Costar Corp., Cambridge, MA) to avoid effects of dust and microbubbles on the quantitative results.

Soft elastic collagen gels were made of gelatin type A (G-2625, Sigma, St. Louis, MO). A 5% collagen gel colored with potassium chromate was used to create a model medium with optical and thermomechanical properties that simulate soft biological tissues better than a water solution. The absorption coefficient of the collagen gel with potassium chromate was very close to the absorption of potassium chromate solution used for gel preparation. The scattering coefficient for the collagen gel at 355 nm was determined from collimated transmission measurements and was found to be equal to 1 cm^{-1} . A fresh pig liver was kept on ice for 6 hours after harvest, then warmed to room temperature and used as an example of soft biological tissue. The measurements were made in gel or tissue slabs with approximate dimensions of 15 mm \times 15 mm \times 3 mm.

Laser Irradiation

The samples were irradiated by a Nd:YAG laser operating in a Q-switched mode (model YG 681, Quantel International, Santa Clara, CA). The experiments were performed at the wavelength of the third harmonic ($\lambda = 355$ nm). The energy of laser pulses was measured with a calibrated joulemeter (ED-200, Gentec, Canada) and equaled 15–30 mJ. A variable aperture was used to produce a homogeneous energy distribution with a tophat profile and a diameter of 1.1–1.4 mm. The temporal profile of laser pulses could be described by a gaussian distribution with a full length at the 1/e amplitude of 14 ns.

The optical properties of the media (absorption, μ_a and effective scattering, μ_s' coefficients) were determined prior to ablation experiments employing the time-resolved stress detection technique with an acoustic transducer and Monte-Carlo simulations assuming the anisotropy factor of 0.9 [14]. It appeared that laser induced heat distribution in media under study were homogeneous in any plane perpendicular to the laser beam (see Discussion). All samples were kept at a stable room temperature (20°C) prior to irradiation. The pulse energy fluence, H_o , incident upon each sample was chosen such that absorbed laser energy density could create a subsurface temperature rise, ΔT , in the range from 10 to 30°C:

$$\Delta T [^\circ\text{C}] = \phi \mu_a [\text{cm}^{-1}] H_o [\text{J}/\text{cm}^2] / \rho [\text{g}/\text{cm}^3] C_v [\text{J}/\text{g}^\circ\text{C}], \quad (1)$$

where ϕ accounts for the effect of diffuse backscattering of light by the medium and ρC_v is the specific heat capacity per unit volume of a medium. For clear solutions and gels, ϕ equals 1. For liver ϕ equals 1.5 for laser beam diameter of 1.1 mm as calculated by the Monte-Carlo code, courtesy of Dr. Lihong Wang.

Methods to Study Ablation

Two methods, time-resolved stress detection and laser-flash photography, were employed to study the phenomena associated with the ablation process inside and outside the irradiated volume. These methods provide complementary information for a better understanding of ablation dynamics.

Time-resolved stress detection with acoustic transducers (models WAT-13 and PAT-01, Science Brothers Inc., Houston, TX) allowed the study of the temporal behavior of stress transients induced in biological tissue or other medium, and the measurement of the recoil momentum transfer upon ablation [15–17]. The absolute pressure magnitude of the plane acoustic waves generated in the irradiated media and propagated along the laser beam axis was calculated (in the absence of diffraction) using measured acoustic transducer signals and calibration parameters described in Oraevsky et al. [14]:

$$P(z') [\text{bar}] = 10(\Gamma/2) \cdot \mu_a [\text{cm}^{-1}] \cdot F_{\text{max}} [\text{J}/\text{cm}^2] \cdot R(z') \cdot T \cdot \Lambda(z') \cdot S, \quad (2)$$

where Γ is the Grüneisen parameter, Λ is the acoustic wave attenuation, R is the stress relaxation function, $T = 1.8$ is the transmittance through the tissue-transducer interface, and S is the detector response. The profile of an acoustic signal is determined by optical and acoustical properties of a medium as well as by the laser irradiation parameters, such as pulse duration, beam diameter, and energy fluence.

Laser-flash photography gave simultaneous imaging of the processes related to the refractive index change, bubble formation inside the irradiated medium, and material ejection above the sample surface. This method yields a real-time picture of the ablation process at various time delays relative to laser energy deposition in the me-

dium. The flash-photography technique consists of two laser pulses synchronized with nanosecond precision [18–20]. In our experiments, an ablative 14-ns pulse at 355 nm from Nd:YAG laser irradiated samples and a second 1-ns pulse of a collimated beam at 650 nm from a nitrogen-pumped dye laser illuminated the field of ablation in a direction perpendicular to the ablative laser pulse for shadow photography. Flash photography was applied to monitor the dynamics of ablation phenomena inside aqueous solutions and above the irradiated surface of aqueous solutions, gels, and tissues.

RESULTS

Figure 1 depicts temporal profiles of stress transients induced by 14-ns pulses of Nd:YAG laser in three media: (1) a clear aqueous solution of potassium chromate, (2) collagen gel, and (3) pig liver. There are two signals presented for each irradiated medium. The profiles marked S correspond to subthreshold laser fluences and those marked G correspond to higher laser fluences that were several times higher than the ablation threshold.

The ablation thresholds were measured at the moment when a slight recoil momentum transfer can be measured by the acoustic transducer [8,9,17]. The initial bipolar positive/negative stress wave is composed of a positive stress due to thermoelastic expansion and a negative stress due to reflection off the air/medium interface. Recoil momentum transfer upon ablation increases the positive stress in a medium and simultaneously diminishes the negative stress amplitude in the acoustic signal (Fig. 1). After the initial bipolar stress transient, there is a sustained positive stress lasting several microseconds, which was caused by the sustained ejection of mass due to surface ablation. The ablation threshold energy density is defined as a product of the incident laser energy and medium absorption coefficient divided by the area of the laser beam. The temperature rise at the ablation threshold calculated using expression (1) did not exceed 30°C in all three cases. The ablation thresholds for the aqueous solution, collagen gel, and pig liver were 20 J/cm³, 38 J/cm³, and 55 J/cm³, respectively, corresponding to temperatures of approximately 5°C, 10°C, and 15°C above room temperature.

Figure 2 demonstrates ablation-associated phenomena that occur within the irradiated solution in the optical zone of energy deposition (Fig.

2a,c) and above the surface of the solution (Fig. 2b,d). The peak temperatures achieved in K₂CrO₄ aqueous solution by the laser pulses were about 40°C, which is substantially below 100°C. There were two distinct stages in the ablation process in water as depicted by the laser-flash photography experiments [8,9]. The first stage was presented as microexplosions with ejection of gas, vapor, and microscopic water droplets. The second stage was the formation of liquid jets.

Figure 3 displays pulsed laser ablation of a collagen gel and a pig liver under confined stress conditions of irradiation. The temperature jump generated in the irradiated volume was about 30°C, yielding a temperature of 51°C, which is substantially lower than that required to achieve boiling or explosive vaporization. However, a significant amount of material was ejected, as seen on the photographs taken 15 μs after the laser pulse.

DISCUSSION

Time-Resolved Detection of Recoil Stress

The initial spatial distribution of pressure is proportional to the spatial distribution of laser energy deposition; however, the pressure wave arriving at a distant pressure transducer can be modified by thermomechanical processes (cavitation and ablation) induced in the medium. The thermal expansion coefficient and the speed of sound in soft tissues are higher than those for water, which leads to a higher Grüneisen coefficient in tissue ($\Gamma = 0.3$ at 20°C) compared with that in water ($\Gamma = 0.12$ at 20°C) [21]. Therefore, similar temperatures in the irradiated volume of aqueous solution and tissue can cause higher pressure amplitudes in tissues. On the other hand, acoustic attenuation in tissues is higher in tissues than in water [22]. We may conclude that laser-induced stress transient pressure and pulse shape at some distance from the point of generation is defined by competitive processes and must be measured or calculated using complex thermodynamic and hydrodynamic equations.

Time-resolved piezoelectric measurements of pressure waves propagating from the distributed pressure source can be analyzed for imaging the laser energy deposition in the optical zone [16] and monitoring modifications of the expected signal due to the onset of momentum transfer caused by ejected material [8–10,15,17].

Thermal expansion of the instantly laser-heated substance causes a significant pressure

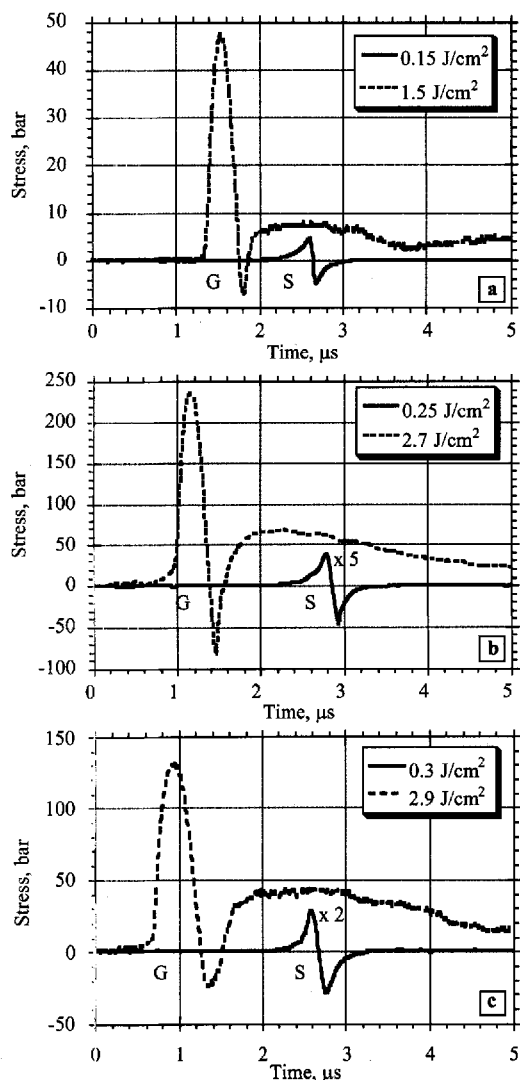


Fig. 1. Temporal profiles of laser-induced stress transients in three water containing media: (a) aqueous solution of potassium chromate, (b) collagen gel, and (c) pig liver. Two Nd:YAG laser fluences were applied for irradiation. S = significantly lower than the threshold of ablation; G = greater than the ablation threshold. S-signals obtained at lower fluences were magnified for better presentation. The position of stress transients does not reflect the time required for the stress to reach the detector but was chosen to make the signals not overlap.

Figure	Absorption, μ_a (cm ⁻¹)	Scattering, μ_s' (cm ⁻¹)	Fluence, H_0 (J/cm ²)	ΔT max (°C)
a	55	0	0.15/1.5	2/20
b	44	~0.1	0.25/2.7	3/30
c	26	28	0.3/2.9	3/30

rise in the irradiated volume. At the onset of heat generation in the irradiated volume, a pressure wave propagates in two axial directions (one to-

ward the surface and the other into the depth of a medium) along the laser beam axis and in a radial direction. As a result of reflection of the stress wave from the boundary between the irradiated medium and the air above it, stress amplitude changes its sign. This converts the plane compression wave into a tensile wave (see Fig. 1, s-profiles). Thermoelastic radial expansion can cause radial compression of a medium with simultaneous circumferential expansion of the medium. All tensile forces in irradiated medium are very important for the ablation process to occur. The onset of cavitation bubbles occurs in aqueous solutions when negative stress exceeds -8 to -14 bar (4 – 6°C temperature jump) [9,19,20]. The threshold depends on the initial number of gas microbubbles and impurities [23]. The negative pressure within the irradiated volume brings the slightly heated medium into a thermodynamically metastable phase, which results in the growth of cavitation bubbles [9]. When the ablation conditions are achieved, intense ejection induces an effective recoil stress that can be detected by acoustic transducer (see Fig. 1). Figure 1 illustrates that the dynamics of the ablation process at temperatures substantially below 100°C are complex. There are two distinct stages of ablation in an aqueous solution. These two stages are less pronounced in collagen gel and liver tissue. The nature of these stages of material ejection was clarified by laser-flash photography [9].

Laser-Flash Photography of Cavitation and Material Ejection

Laser-flash photography can be applied to monitor processes associated with ablation both within the optical zone and above the irradiated surface only in clear media (aqueous solutions and gels). Nevertheless, clarification of the ablation mechanisms for the model systems provides very useful information, which can be applied as a "first-approximation" to soft biological tissues.

Photographs taken at two various time delays ($1 \mu\text{s}$ and $15 \mu\text{s}$) relative to ablative laser pulses depict phenomena of inception, expansion, coalescence, and collapse of cavitation bubbles. A comparison of processes above and beneath the surface under ablation helps to understand the two stages of liquid ejection. The process of material ejection is statistical. The first stage is associated with expansion of cavitation bubbles incepted in the optical zone during the propagation of the expansion phase of a stress transient. A

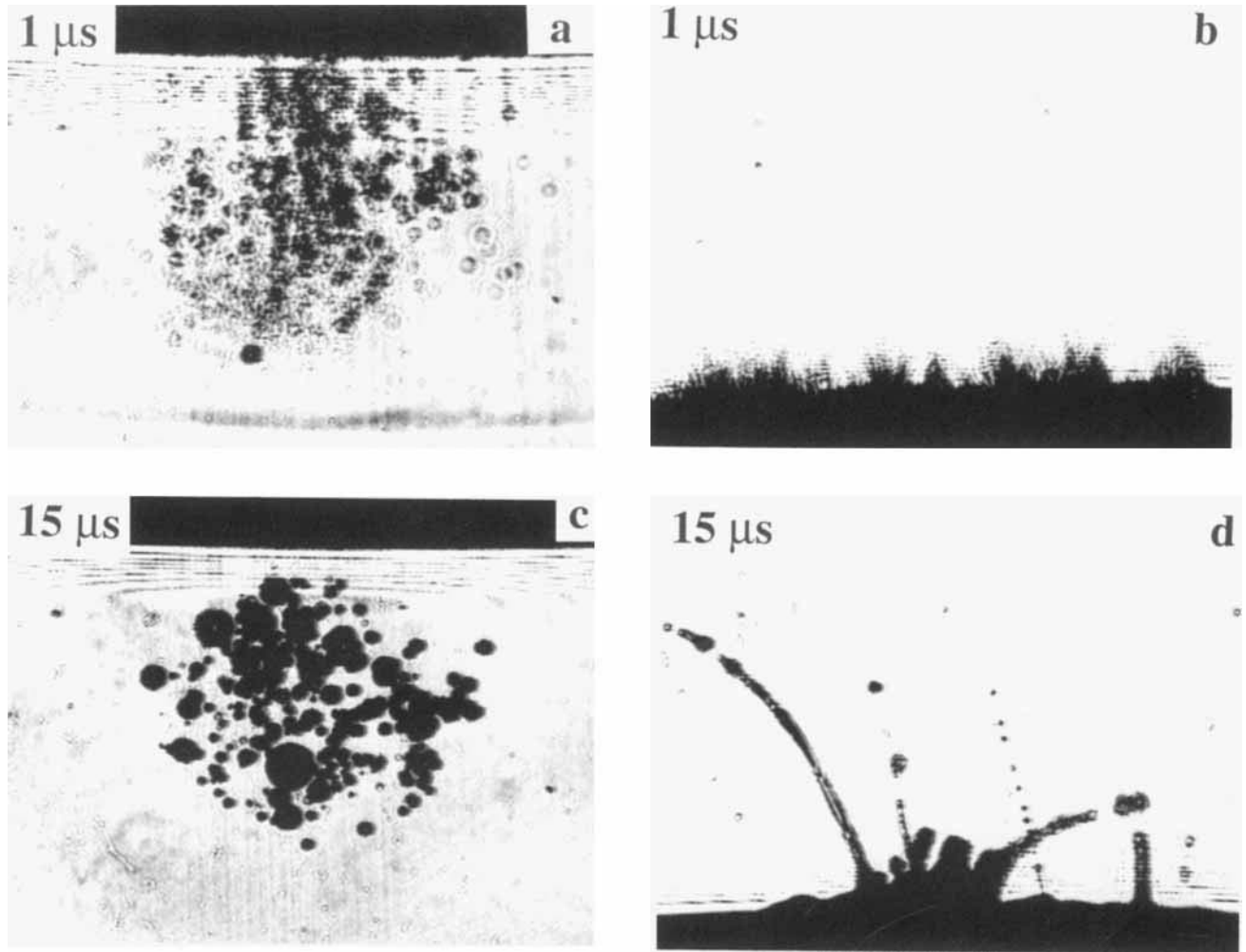


Fig. 2. Ablation events depicted by laser-flash photography beneath the irradiated surface (a,c) and above the surface (b,d) of potassium chromate (K_2CrO_4) aqueous solution.

Figures	Beam diameter (mm)	Absorption, μ_a (cm^{-1})	Fluence, H_o (J/cm^2)	ΔT max ($^{\circ}C$)
a and c	1.4	50	1.23	15
b and d	1.4	56	1.85	26

Delay times between the 14-ns Nd:YAG laser pulse and the 1-ns dye-laser pulse are shown on each photo.

gradient between the compression and extension phase is presented in Figure 2a as a horizontal white-and-black striped line at (see the bottom of Fig. 2a). The white line corresponds to the compression phase that caused the refractive index of liquid to increase, and the black stripe on this line represents a tensile wave that created a volume of liquid with a decreased refractive index. Figure 2b displays the first ablation stage at the surface where separate cavitation bubbles expand and rupture. Expansion of cavitation bubbles is able

to eject material only from a thin subsurface layer of an aqueous solution. The second stage of ablation is stimulated by collapse of cavitation bubbles (see Fig. 2b,d). Coalescence of small cavitation bubbles into bigger bubbles with subsequent collapse of these large bubbles can generate shock waves and, more importantly, substantial hydrodynamic motions directed toward the surface [24,25]. Collapse of a large bubble leads to water mass motion into the volume occupied by that bubble to yield a water jet similar to the water jet

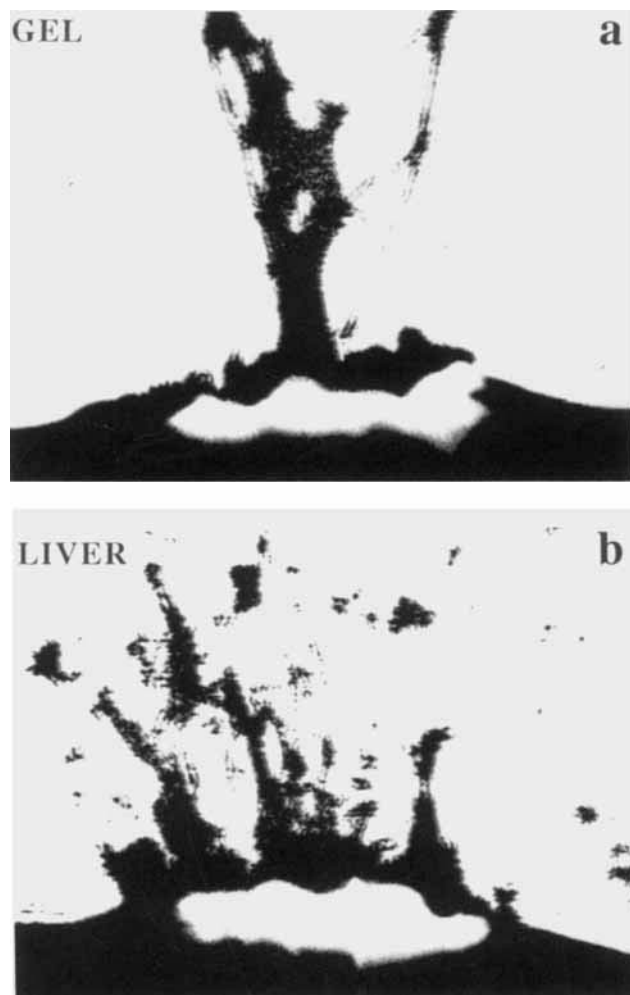


Fig. 3. Material ejection upon Nd:YAG pulsed laser ablation at 355 nm of collagen gel (a) and a pig liver (b).

Figures	Beam diameter (mm)	μ_a/μ_s' ($\text{cm}^{-1}/\text{cm}^{-1}$)	Fluence, H_0 (J/cm^2)	ΔT max ($^{\circ}\text{C}$)
3a	1.1	44/~0.1	2.7	30
3b	1.1	26/28	3.1	30

Microphotographs are taken 15 μs after nanosecond ablative laser pulses.

produced when a stone is thrown in water (see Fig. 2d). Propagation of the shock waves toward the surface with subsequent reflection from the free surface also may cause strains and ejection of liquid jets.

Images of ejecta obtained for collagen gel and biological tissue (liver) can be compared with ablation pictures of aqueous solution (see Fig. 3). There is a certain similarity of irradiation parameters required for ablation of all three me-

dia. There is an efficient ablation that occurs in all media at temperatures substantially below 100°C. In all three cases ablation requires an expansion of irradiated volume. The tensile magnitudes required for ablation are slightly different for various media. Different water content and mechanical properties of the studied media cause the total duration of the ejection and the shape of ejecta to be different. However, similar threshold temperatures and negative pressures required to initiate ablation are evidence that the basic mechanisms underlying ablation processes under confined-stress conditions are similar for aqueous solutions, collagen gels, and soft biological tissues.

Ablation Mechanism for Water Containing Media Under Confined Stress Irradiation Conditions

Previously reported thermal models are found to contradict the experimental observations of short-pulse laser ablation of soft tissues [26]. The model that depicts some important features of pulsed laser ablation under confined-stress conditions is the model of front-surface spallation [4]. This model demonstrates the importance of the thermoelastic expansion of an instantly heated tissue volume. The term *laser front-surface spallation* has been introduced in Dingus and Scammon [4] to describe tissue ejection induced by thermoelastic expansion and stress reflection to yield a negative stress wave whose magnitude exceeds the tensile strength of a tissue. Such a one-dimensional hydrodynamic approach to the description of ablation is more appropriate for hard materials than for water-containing media [27].

The kinetics of the short-pulse laser ablation of water-containing media is more complicated than that described by the spallation model. The process of spallation occurs not later than the moment when the irradiated volume expands to its maximal new dimensions. This time can be calculated as the effective light penetration depth divided by the speed of sound in the medium. For example, at an effective light penetration depth of $\delta \approx 100 \mu\text{m}$ in liver for an excimer laser at 308 nm, and given that the speed of sound in liver is about $1.57 \times 10^5 \text{ cm/s}$, it takes about 70 ns for the complete expansion of the irradiated volume. Therefore, spallation may be described as a process of tissue rupture delayed not more than 70 ns against the moment of laser energy deposition. In contrast to the simple front-surface spallation model, our experimental results demonstrated that material ejection is a long-duration process

that starts after 100 ns, changes its nature after 5–10 μs , and proceeds for many hundreds of microseconds. Qualitative observation of the ablation process with laser-flash photography quantitatively supported by the time-resolved detection of stress transients, helped in gaining an understanding of the kinetics of short-pulse laser ablation [8,9]. At laser fluences that do not substantially exceed the ablation threshold, ejection occurs as a two-stage statistical process. During the first several microseconds, ablation is observed as microdisruptions of individual subsurface bubbles. The second stage lasts from several tens of microseconds (in tissues) to several hundreds of microseconds (in water) and can be described as ejection of larger volumes (jets) of material, produced due to collapse of large cavitation bubbles in the volume of irradiated medium. The thermodynamics of laser tissue ablation is extremely complex and involves numerous forces that can be induced in heated water-containing media and play a role tissue ablation.

Ablation at temperatures below 100°C requires a free (unconstrained) surface (e.g., an air/medium interface). A rigid surface, produced, for example, by an attached optical fiber, will prohibit “cold” cavitation-based ablation. Even a relatively thin water layer on a tissue surface may cause an increase in the ablation threshold. Tissue optical properties may also strongly affect the ablation-threshold temperature. High optical attenuation may yield poor stress confinement in an irradiated volume and lead to higher temperatures of ablation. Three-dimensional consideration of laser-induced transient stress revealed long-lived circumferential and shear components of tensile stress induced in media upon pulsed laser irradiation with a tophat radial intensity distribution [28,29]. Negative circumferential and shear stress are independent of acoustic mismatch at the tissue boundary. However, these stresses have 5–10 times lower magnitude and occur only in the ring at the tissue surface around the irradiated area. Therefore, this type of negative stress may support material ejection from the peripheral ring around the irradiated area ablated with fibers but not induce cavitation in the irradiated volume.

Role of Microheterogeneities in Laser Absorption and Laser Ablation

Our experiments demonstrated ablation of water-containing media at temperatures substantially below 100°C. The thermal energy distribu-

tion in aqueous potassium chromate was homogeneous under the chosen experimental conditions. Optical absorption by potassium chromate solvated in water is heterogeneous, and the initial heat is located (at a subnanosecond time scale) in the small volume (about 1 nm in diameter) of chromate surrounded by several water molecules of the solvating shell. However, after a 10-ns laser pulse heat is evenly distributed between any two given chromophores in the irradiated volume. The role of heterogeneous absorption in tissue ablation by short laser pulses was studied by Oraevsky et al. [30]. Simple estimates are given later to support our conclusion that optical microchromophore centers play a negligible role in the thermodynamics of ablation by laser pulses longer than 10 ns in duration.

The concentration, C , of potassium chromate used in our experiments was 1–2 mg/cm^3 , which for the molecule of K_2CrO_4 , with a molecular weight of 194, means $C = (5\text{--}10) \cdot 10^{-3} \text{ M} = (3\text{--}6) \cdot 10^{18} \text{ molecules}/\text{cm}^3$. Therefore, the distance, d , between dissolved molecules equals 5–7 nm. To obtain an average temperature jump in the subsurface layer of irradiated medium of 25°C one needs 100 J/cm^3 of absorbed laser energy density, which means $1.79 \cdot 10^{20} \text{ photons}/\text{cm}^3$ at a photon energy $hc/\lambda = 5.59 \cdot 10^{-19} \text{ J}$ (355-nm wavelength). This yields 15–30 absorbed photons per dissolved molecule of potassium chromate per laser pulse. The time required for the heat diffusion process in water-containing media to move thermal energy from one chromophore center to another (a distance of 6 nm) is equal to

$$\tau_{HD} = \frac{d^2}{4\chi} = \frac{(6 \cdot 10^{-7} \text{ cm})^2}{4 \cdot 1.3 \cdot 10^{-3} \frac{\text{cm}^2}{\text{s}}} = 6.9 \cdot 10^{-11} \text{ s}. \quad (3)$$

Therefore, thermal heterogeneities (superheated microchromophore centers) exist in an irradiated volume for only 70 ps. For a 14-ns laser pulse this means that before the next photon is absorbed in solution by a given chromophore, the heat generated in the solvated chromophore (assume a 10 Å radius or 10^{-7} cm),

$$E_{\text{chrom}} = \frac{6 \cdot 10^{-19} \text{ J/photon}}{\frac{4\pi}{3} (1 \cdot 10^{-7} \text{ cm})^3} = 143 \text{ J}/\text{cm}^3, \quad (4)$$

should diffuse out. Furthermore, E_{chrom} yields a

maximal temperature-rise in a microchromophore of only about 35°C, which is still under 100°C.

Our experiments demonstrated that ablation under confined-stress conditions of irradiation can be described as follows. Instant laser heating (compared with the time of stress relaxation) allows for the generation of high-magnitude compression without a pronounced temperature rise followed by thermoelastic expansion of the irradiated volume. Thermoelastic tension in the heated volume creates the necessary conditions for the inception and expansion of cavitation bubbles. Rupture of single subsurface bubbles yields the initial removal of a small volume of material. Coalescence of small cavitation bubbles into larger bubbles allows for the accumulation of substantial energy. Collapse of these large bubbles can generate intense hydrodynamic motions directed toward the surface that produce jets of ablated material. In addition, bubble collapse releases the accumulated energy and produces shock waves [31]. Shock waves directed toward a free surface can strain this surface and also slightly contribute to mass ejection.

CONCLUSION

The negative phase of stress transients upon ablation was found to play an important role in the thermodynamics of pulsed laser ablation under confined-stress conditions. A fast initial compression of the irradiated volume followed by a rarefaction phase creates the necessary conditions for cavitation that yields ablation at temperatures substantially below 100°C. Based on experimental data, the ablation process in water-containing media upon short-pulse laser irradiation was found to involve two stages of material ejection: (1) due to the expansion and (2) due to the collapse of cavitation bubbles. Ablation at sub-boiling temperatures is delayed against a laser pulse. The minimal delay is equal to the time it takes for the tensile stress to reach the spallation threshold. When laser fluence is high enough to make the temperature of the irradiated volume exceed 100°C, tensile forces are not required for ablation. Cavitation (bubble formation) can occur even during laser energy deposition under positive pressure (≥ 1 atm) and can be described by a model of thermal explosion (intense boiling). Ablation at temperatures below 100°C requires a free (unconstrained) surface (e.g., air/medium interface), which efficiently reflects thermoelastic

stress propagating in tissue along the laser beam axis. Thermal explosion is more effective for tissue removal compared with "cold" photomechanical ablation. On the other hand, thermal-explosion-induced ablation is always associated with substantial recoil stress and high-amplitude shock waves, which may cause significant mechanical damage at the cellular level [32–34]. Ejection of an ablation plume upon "cold" cavitation driven ablation proceeds with a much lower initial velocity, and as a result, with a lower amplitude of recoil stress. Therefore, pulsed laser ablation under confined-stress conditions of irradiation minimizes thermal injury to adjacent tissues, because it may occur at temperatures below 100°C and involves lower magnitude stress transients and recoil pressure waves.

ACKNOWLEDGMENTS

This research was supported by the Whitaker Foundation, the Department of Energy Center of Excellence, and the National Institute of Health, grant R29-HL45045.

REFERENCES

1. Oraevsky AA, Esenaliev RO, Letokhov VS. Pulsed laser ablation of biotissue. Review of ablation mechanisms. In: Miller JC, ed. "Lecture notes in Physics." Berlin: Springer-Verlag 1991. Proceedings of the Workshop "Laser Ablation: Mechanisms and Applications," April 1991, Oak Ridge, Tennessee.
2. Isner JM, Clarke RH. The paradox of thermal laser ablation without thermal injury. *Lasers Med Sci* 1987; 2: 165–173.
3. Jacques S. Role of tissue optics and pulse duration on tissue effects during high power laser irradiation. *Appl Optics* 1993; 32:2447–2454.
4. Dingus RS, Scammon RJ. Grüneisen stress induced ablation of biological tissue. *SPIE* 1991; 1427:45–54.
5. Dingus RS, Curran DR, Oraevsky AA, Jacques SL. Microscopic spallation process and its potential role in laser-tissue ablation. *SPIE* 1994; 2134A:434–445.
6. Venugopalan V, Nishioka NS, Mikic BB. The effect of laser parameters on the zone of thermal injury produced by laser ablation of biological tissue. *Trans ASME* 1994; 116:62–70.
7. Schomacker KT, Domankevich Y, Flotte TJ, Deutsch TF. CO:MgF laser ablation of tissue. Effect of wavelength on ablation threshold and thermal damage. *Lasers Surg Med* 1991; 11:141–151.
8. Oraevsky AA, Jacques SL, Tittel FK. Pulsed laser ablation mechanism of water containing media under confined stress conditions studied by time-resolved stress detection and flash-photography. In: Dingus R, ed. "Dynamic Response of Materials to Pulsed Heating," Los Alamos Conference Proceedings, 1993.
9. Oraevsky AA, Jacques SL, Tittel FK. Pulsed laser abla-

- tion mechanism of water containing media under confined stress conditions studied by time-resolved stress detection and flash-photography, *J Appl Phys* 1995; 78(2): 1–10.
10. Oraevsky AA, Jacques SL, Tittel FK, Henry PD. Pulsed laser ablation of atherosclerotic aorta. Relative role of thermal and mechanical effects. *Lasers Surg Med* 1993; 5(Suppl):11–12.
 11. Van Leeuwen TG, Jansen ED, Motamedi M, Welch AJ, Borst C. Bubble formation during laser ablation: Mechanism and implications. *Proc. SPIE* 1993; 1882:13–22.
 12. Oraevsky AA, Jacques SL, Pettit GH, Saidi I, Tittel FK, Henry PD. XeCl laser ablation of aorta tissue: Optical properties and energy pathways. *Lasers Surg Med* 1992; 12:585–597.
 13. Van Leeuwen TG, Jansen ED, Motamedi M, Welch AJ, Borst C. Excimer laser ablation of soft tissue: A study of content of rapidly expanding and collapsing bubbles. *IEEE J Quant Electron* 1994; 30:1339–1345.
 14. Oraevsky AA, Jacques SL, Tittel FK. Determination of tissue optical properties by time-resolved detection of laser-induced stress waves. *Proc. SPIE* 1993; 1882:86–101.
 15. Cross FW, Al-Dhahir RK, Dyer PE, MacRobert AJ. Time-resolved photoacoustic studies of vascular tissue ablation at three wavelengths. *Appl Phys Lett* 1987; 50:1019–1021.
 16. Oraevsky AA. A nanosecond acoustic transducer with applications in laser medicine. *IEEE/LEOS Newslet* 1994; 8:6–17.
 17. Esenaliev RO, Oraevsky AA, Letokhov VS, Karabutov AA, Malinsky TV. Studies of acoustic and shock waves in the pulsed laser ablation of biological tissue. *Lasers Surg Med* 1993; 13:470–484.
 18. Paltauf G, Schmidt-Kloiber H. Time-resolved observation of thermal and mechanical effects in tissue models induced by short laser pulses from an optical parametric oscillator. *Proc. SPIE* 1993; 2077:25.
 19. Paltauf G, Reichel E, Schmidt-Kloiber H. Study of different ablation models by use of high-speed-sampling photography. *Proc. SPIE* 1992; 1646:343–352.
 20. Jacques SL, Gofstein G, Dingus RS. Laser flash-photography of laser induced spallation and mechanical stress waves. *Proc. SPIE* 1992; 1646:284–294.
 21. Duck FA. "Physical Properties of Tissue." London: Academic Press, 1990.
 22. Goss SA, Johnston RL, Dunn F. Comprehensive compilation of empirical ultrasonic properties of mammalian tissues. *J Acoustic Soc Am* 1978; 64:423–457.
 23. Couzens DCF, Trevena DH. *Nature* 1969; 222:473–474.
 24. Vogel A, Lauterborn W. Time-resolved particle image velocimetry used in the investigation of cavitation bubble dynamics. *Appl Optics* 1988; 27:1869–1876.
 25. Esenaliev RO, Karabutov AA, Podymova NV, Letokhov VS. Laser ablation of aqueous solutions with spatially homogeneous and heterogeneous absorption. *Appl Phys B* 1994; 59:73–81.
 26. Dmitriev AK, Furzikov NP. Mechanism of laser ablation of biological tissue. *Sov Phys Izvestiya* 1989; 53:1105–1110.
 27. Curran DR, Seaman L, Shockey DA. Dynamic failure of solids. *Phys Reports* 1987; 147:254–269.
 28. Albagli D, Dark M, Rosenberg C, Perelman L, Itzkan I, Feld MS. Laser-induced thermoelastic deformation. A three dimensional solution and its application to the ablation of biological tissue. *Med Phys* 1994; 21:1323–1331.
 29. Boehm R, Rich J, Webster J, Janke S. Thermal effects and surface cracking associated with laser use on human teeth. *Trans ASME, J Biomechan Eng* 1977; 11:189–194.
 30. Oraevsky AA, R.O. Esenaliev VS, Letokhov VS. Temporal characteristics and mechanism of atherosclerotic tissue ablation by picosecond and nanosecond laser pulses. *Lasers Life Sci*, 1992; 5:75–93.
 31. Trevena DH. "Cavitation and tension in liquids." Bristol: Adam Hilger Press, 1987.
 32. Doukas AG, McAuliffe DJ, Flotte TJ. Biological effects of laser-induced shock waves: Structural and functional cell damage in vitro. *Ultrasound Med Biol* 1993; 19:137–146.
 33. Jansen DE, Tuong HL, Welch AJ. Excimer, Ho:YAG, and Q-switched Ho:YAG ablation of aorta: A comparison of temperatures and tissue damage in vitro. *Appl Optics* 1993; 32:526–534.
 34. Cummings JP, Walsh JT. Tissue tearing caused by pulsed laser-induced ablation pressure. *Appl Optics* 1993; 32: 494–503.